phys. stat. sol. (a) **201**, No. 2, 345–352 (2004) / **DOI** 10.1002/pssa.200303971

Quantum dot semiconductor lasers with optical feedback

G. Huyet[*,1], **D. O'Brien**[1], **S. P. Hegarty**[1], **J. G. McInerney**[1], **A. V. Uskov**[2], **D. Bimberg**[3], **C. Ribbat**[3], **V. M. Ustinov**[4], **A. E. Zhukov**[4], **S. S. Mikhrin**[4], **A. R. Kovsh**[4], **J. K. White**[5], **K. Hinzer**[5], and **A. J. SpringThorpe**[6]

[1] Physics Department, National University of Ireland, University College Cork, Cork, Ireland
[2] NMRC, National University of Ireland, University College Cork, Lee Malting, Cork, Ireland
[3] Institut für Festkörperphysik, Technische Universität Berlin, Germany
[4] A. F. Ioffe Physico-Technical Institute, Russian Academy of Sciences, St. Petersburg, Russia
[5] Bookham Technology, 3500 Carling Ave., Ottawa, On, Canada
[6] National Research Council Canada, Institute for Microstructural Sciences, Ottawa, On, Canada

Received 19 September 2003, accepted 17 November 2003
Published online 14 January 2004

PACS 42.55.Px, 78.67.Hc

We analyse the sensitivity of quantum dot semiconductor lasers to optical feedback. While bulk and quantum well semiconductor lasers are usually extremely unstable when submitted to back reflection, quantum dot semiconductor lasers exhibit a reduced sensitivity. Using a rate equation approach, we show that this behaviour is the result of a relatively low but nonzero line-width enhancement factor and strongly damped relaxation oscillations.

1 Introduction The performance of quantum dot devices is presently the subject of great interest [1]. In particular, several studies have concentrated on the sensitivity of quantum dot semiconductor lasers to the influence of optical feedback [2, 3]. Unlike bulk or quantum well semiconductor lasers, these devices have symmetric gain curves [1] and experiments [4] have demonstrated very small phase-amplitude coupling (α-parameter). As the extra sensitivity of semiconductor lasers to feedback is governed to a large extent by the non-zero value of α, it is thought they could have feedback characteristics different to bulk semiconductor and quantum well lasers. This has brought the possibility of designing directly modulated semiconductor lasers operating without optical isolators and therefore reducing the cost of these devices.

In this paper, we investigate quantum dot lasers with external optical feedback. We first review the properties of semiconductor lasers under the influence of optical feedback. Then we present measurements of the line-width enhancement factor and the relative intensity noise spectrum of these devices before showing the reduced sensitivity to optical feedback of quantum dot semiconductor lasers compared to quantum well semiconductor lasers. In the last part of the paper, we provide a Lang-Kobayashi type model and provide an explanation for the reduced sensitivity to optical feedback.

2 Dynamics of semiconductor lasers with optical feedback External cavity semiconductor lasers were first considered in order to narrow the natural laser linewidth. However it was also observed that, for some parameter regimes, the re-injection of light into the main resonator generates instabilities. The laser may, for example, operate with several external cavity modes and the relative intensity noise

[*] Corresponding author: e-mail: huyet@physics.ucc.ie, Phone: +353 21 490 23 81, Fax: +353 21 427 69 49

exhibits a series of peaks at multiples of the external round trip frequency. Feedback can also induce self sustaining relaxation oscillations and even Low Frequency Fluctuations (LFF) [5]. Since these early works the origin of the LFF regime has been the subject of great interest both theoretically and experimentally. Partly this interest stems from the original motivation of improving the laser characteristics, but is also due in part to a desire to understand the high-dimensional non-linear dynamics of the time-delayed systems. In the early 80's, experimental investigations have concentrated on linewidth properties [8–11] and radio frequency fluctuations with and without modulation of the injection current [12, 13]. It was also experimentally shown that LFF are closely related with fluctuations at higher frequency such as the external cavity frequency and the solitary laser relaxation rate [14]. In this last article, it was shown that the power drop-outs occur randomly and are followed by a slow recovery of about 10 steps, each of them corresponding to an external cavity round trip. The coherence properties were analysed by Lenstra et al. [15] who found a line broadening up to 25 GHz. For this reason, this instability is also refered to as the ''Coherence Collapse" (CC) regime. A classification of laser behaviour vs the control parameters was first performed by Tkach and Chraplyvy [16] who identified five different regimes. Regime I corresponds to low feedback level were broadening or narrowing of the optical linewidth is observed depending on the feedback phase, regime II to mode hopping between several external cavity modes and regime III to stable emission for higher feedback level. Regime IV, which is observed for higher feedback levels, is associated with the Coherence Collpase and regime V to stable emission with a narrow linewidth at high feedback levels. However regime IV should be divided in three different sub-regimes: first the Low Frequency Fluctuation regime where power drop-outs can be distinctively observed; second the coherence collapse regime and third bistability between stable emission and the LFF and the CC regime. This last sub-regime, which was, for instance, reported in ref. [17–19] occurs at the boundary of regime V. The model commonly used to describe the dynamics of external cavity lasers is the model developed by Lang and Kobayashi [7]. This model describes the laser with rate equations for the complex amplitude of the electric field and for the carrier density (population inversion). The optical feedback was accounted for by adding a term in the field equation corresponding to the re-injection of a portion of the field, delayed by an external cavity round-trip. In this paper we will use the following dimensionless form of these equations:

$$\begin{aligned} \dot{E} &= \kappa(1+i\alpha)\,(N-1)\,E + \gamma e^{-i\varphi_0} E(t-\tau), \\ \dot{N} &= -\frac{1}{T}\,(N - J + |E|^2 N)\,, \end{aligned} \tag{1}$$

where E is the complex amplitude of the electric field, N is the carrier density, κ is the field decay rate, T is the carrier decay time, α is the linewidth enhancement factor, γ represents the feedback level, J is the pumping parameter, φ_0 is the feedback phase when the laser emits at the solitary laser frequency ω_0, and τ is the external cavity round trip time, implying that $\varphi_0 = \omega_0\tau$. It is worthwhile to note that these equations assume single laser mode operation and neglect re-injection of light after multiple reflections in the external cavity.

The steady-state solutions of these equations correspond to external cavity modes and other unstable solutions sometimes referred to as antimodes. They are associated with a destructive interference between the emitted field and the re-injected field (in the limit where $\alpha = 0$) and are therefore unstable. The number of external cavity modes depends on the parameter $C = \gamma\tau\sqrt{1+\alpha^2}$ [15]. If $C > 1$ there is more than a single solution and if $C \gg 1$ there are approximately $\frac{C}{\pi} + 1$ external cavity modes. The stability of these solutions has been addressed by several authors [20–24] and it was found that external cavity modes can become unstable as relaxation oscillations become undamped and the laser displays self-sustained pulsations. For example, Helms and Petermann defined the onset of self pulsations as when the damping rate of the relaxation oscillations is $\Gamma = \gamma\sqrt{1+\alpha^2}$, showing that the α parameter is not the only critical parameter defining the sensitivity to optical feedback. The behaviour of semiconductor lasers in the unstable regime has been the subject of many experimental,

numerical and theoretical investigations. Numerical simulations [25] of the LK equations have shown that the LFF regime is the result of a chaotic itinerancy between destabilised external cavity modes. It was later shown for this model that the power exhibits strong irregular picosecond light pulses at a rate associated with the relaxation oscillation frequency [26]. These results were explained by reducing the dynamics to a three dimensional dynamical system [27]. Fast pulses in the laser intensity have also been observed [28, 29] for both multimode [30] and single mode [31] lasers.

3 The experiment The sensitivity of quantum dot semiconductor lasers was investigated using semiconductor lasers emitting at around 1.3 μm. Both the QD and QW lasers were as-cleaved Fabry–Pérot ridge waveguide devices. The cavity length was 1.5 mm, and both devices operated predominately in a single lateral mode. The QDL ridge width was 7 μm and the QWL ridge width was 2.4 μm. The active region of the QDL consisted of a five-fold stack of InGaAs QDs in a GaAs waveguide, while the quantum well laser had six 6 nm AlGaInAs QWs as its active region. The detailed QWL and QDL growth and fabrication conditions are described elsewhere [32, 33]. The line-width enhancement factor for both devices was measured using the Hakki–Paoli method. The lasers were run in the pulsed regime to avoid thermally induced wavelength shifts. From these measurements, we obtain an alpha factor of 1.6. The same measurement carried out with the quantum well devices gives alpha 3–5. The Relative Intensity Noise (RIN) was measured in the CW regime. The devices were pumped using an ILX LDX3235 current driver with stability of 50 ppm. All measurements were conducted at 20 °C, the laser mount temperature being maintained using a Newport 350 TEC. The light was coupled to a Newport (D30) detector after passing through an optical isolator providing isolation of 40 dB. The signal was amplified using a Miteq high gain amplifier and analysed with an Advantest R3172 electronic spectrum analyzer (ESA). The D30 had a bandwidth of 14 GHz, the ESA a bandwidth of 26 GHz and the Miteq amplifier had a bandwidth of 20 GHz and a noise figure of 3.5 dB. The QWL demonstrated an archetypal RIN spectrum with a well defined peak near the relaxation oscillation frequency. RIN spectra for different operating points of the QDL are presented in Fig. 1. The QDL never shows a clear relaxation oscillation at any operating point. The suppressed peak is clear evidence of overdamping of the relaxation oscillation, a conclusion supported by transient measurements on similar devices [34]. To analyse the effect of optical feedback on these devices, a broadband coated Al mirror was mounted 45 cm from the laser, the lens being adjusted so as to position the beam waist at the mirror for maximal coupling. In order to vary the level of feedback into the device, a variable neutral density filter (ND) was placed in the external cavity. A beam splitter was used to couple a fraction of the beam to the diagnostic instruments. Again, in order to avoid extraneous feedback from the diag-

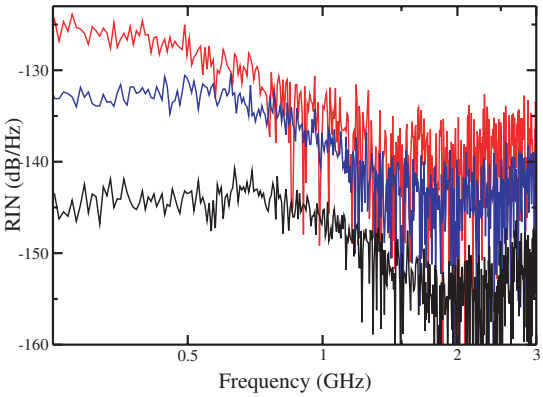

Fig. 1 (online colour at: www.interscience.wiley.com) RIN spectra of the QD lasers for different drive currents. From uppermost to lowermost: 130 mA, 140 mA, 190 mA.

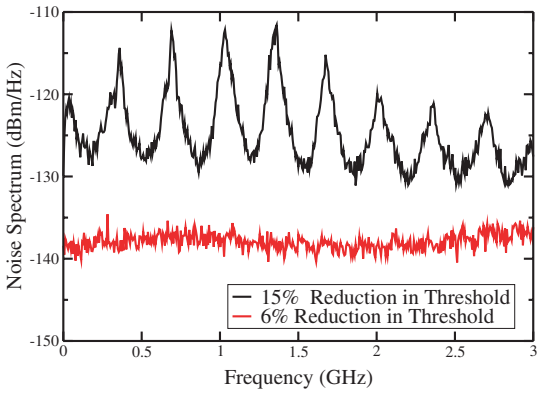

Fig. 2 (online colour at: www.interscience.wiley.com) Noise spectra of QD laser under different feedback conditions. Lower curve is for 6% reduction in threshold and upper curve is 1% reduction in threshold.

nostics, an isolator was positioned after the beamsplitter. A second lens coupled the diagnostics beam to a short length of fiber which guided the light to a Newport D30 fast detector. The electronic spectrum was measured at different feedback levels and pump currents. Stability of the output of the laser was assessed from the presence or absence of RF and microwave components in the photodiode signal. When present these peaks tended to be particularly pronounced at multiples of the round-trip frequency ($\sim$330 MHz). For strong feedback levels, the feedback strength was deduced from the amount of threshold reduction using a linear gain approximation, in a method similar to Olsson [35]. For weaker feedback levels, the transmittance of the external cavity filters was used to calculate the feedback level. In an effort to clarify the experimental data, a stability criterion was introduced. If any component of the microwave spectrum exceeded -130 dB m/Hz, the laser operating point was recorded as unstable. If no part of the spectrum exceeded this level, the operating condition was recorded as stable. This criterion corresponded to a maximum RIN < -136 dB/Hz when the laser emits 1 mW. Two sample microwave spectra are shown in Fig. 2. These are recorded for the same QDL, operating at 1.25 times threshold, with different threshold reductions. The cavity was kept the same for all data. In the lower curve (6% threshold reduction), the microwave spectrum is simple broadband noise (in fact amplifier noise), and the max level is < -135 dB m/Hz. Therefore this operating point is stable. For the upper curve (15% threshold reduction), the microwave spectrum consists of broadened peaks at every round trip frequency multiple within the trace bandwidth. As virtually every frequency exceeds the -130 dB m/Hz criterion this operating point is classed as unstable. This procedure was repeated as a function of the driving current and the feedback level for both the QDL and the QWL. In previous work that has carried out similar parameter space mappings, multiple regime classes have been used, including Low Frequency Fluctuations, Coherence Collapse and at very high feedback levels, linewidth narrowing [37]. In this experiment, where the laser facets had no anti-reflection coatings, the laser never recovered stability with the injection fixed and the feedback level increased. Also, all types of intensity instability were grouped together as an unstable operating condition. Thus, our stability diagram for each type of laser simplified to a boundary separating stable operation from unstable operation. This diagram is shown in Fig. 3. The result for the QWL is broadly in line with the literature (see for example [36, 37] and refs therein). The QDL however maintains its stability at much greater levels of feedback, up to 30 dB greater at some operating points.

4 The model In quantum dot semiconductor lasers, the carriers are first injected into a quantum well before being captured into the quantum dot as previously used in other models describing QD laser

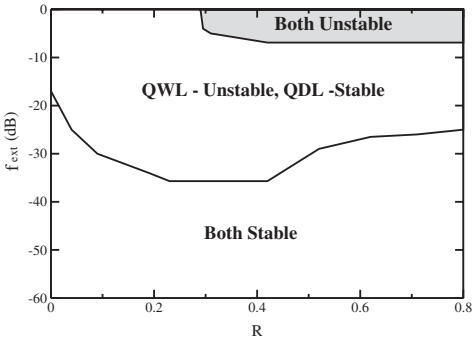

Fig. 3 Stability diagram of the external feedback level f_{ext} versus the pump parameter $R = I/I_{\text{th}} - 1$. f_{ext} is the ratio of power returned to the facet divided by the power emitted, including all coupling losses.

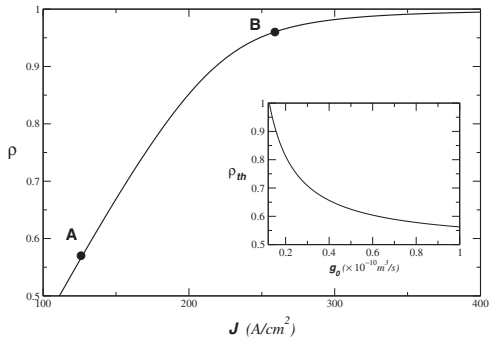

Fig. 4 QD occupation probability ρ versus the drive current J. How the operating point of the laser varies as g_0 changes is shown inset. The two different operating points investigated are shown, (A and B). $C = 10^{-20}$ m^4/s, $R_{\text{esc}} = 0$, $B = 0$, $N_d = 2 \times 10^{15}$ m^{-2}, $\vartheta = 2.4 \times 10^{22}$ m^{-3}, $\tau_n = \tau_d = 1$ ns and $\tau_s = 3$ ps.

dynamics [38, 40], we write one equation for the population in the dots and one equation for the population in the well. We neglect coupling between dots and the influence of inhomogeneous broadening as these are not essential features for the physics described in this paper. With these approximations, the system can be described using the following rate equations:

$$\begin{aligned}
\dot{E} &= -\frac{E}{2\tau_s} + \frac{g_0 \vartheta}{2}(2\rho - 1)E + i\frac{\delta\omega}{2}E + \frac{\gamma}{2}E(t-\tau), \\
\dot{\rho} &= -\frac{\rho}{\tau_d} - g_0(2\rho - 1)|E|^2 + F(N,\rho), \\
\dot{N} &= J - \frac{N}{\tau_n} - 2N_d F(N,\rho),
\end{aligned} \tag{2}$$

where E is the complex amplitude of the electric field, N is the carrier density in the well, ρ is the occupation probability in a dot, τ_s is the photon lifetime, τ_n and τ_d are the carrier lifetime in the well and the dot respectively, N_d is the 2D density of dots and J is the pump. $g_0 = \sigma_{\text{res}}\nu_g$, where σ_{res} is the cross section of interaction of carriers in the dots with photons, ν_g is the group velocity, $\vartheta = \dfrac{2N_d\Gamma}{d}$, where Γ is the confinement factor and d is the thickness of the dot layer [40]. The parameters γ and τ describe the feedback level and delay time. The function $F(N,\rho)$ describes the rate of exchange of carriers between the well and the dots. Carrier capture and escape from the dots can be mediated through carrier-phonon or through carrier-carrier (Auger) interaction. In its most general form, $F(N,\rho) = R_{\text{cap}}(1-\rho) - R_{\text{esc}}\rho$, where $R_{\text{cap}} = CN^2 + BN$. The constants B and C describe the carrier-phonon and Auger carrier capture respectively. R_{esc} is a temperature dependent function controlling carrier escape from the dots. From a phenomenological viewpoint, the refractive index of the device depends on the carrier densities in the well and/or dots. If we assume linear dependencies, the variation of the laser frequency with these densities reads $\delta\omega = \beta_1 N + \beta_2\rho$. The coefficient β_1 describes the plasma effect from the carriers in the well, while β_2 describes the variations due to the population in the dots. If the dots are described by two-level atoms with symmetric line shape, then $\beta_2 = 0$ from the Kramers–Kronig relations. However more complex effects [39], such as Coulomb interactions can lead to nonzero values for β_2.

We first consider the properties of the laser without optical feedback. In this case the evolution of the intensity and carrier densities do not depend on the phase of the electric field and, as a result, Eq. (2) can be rewritten with the photon density S and the carriers densities. An important feature of these equations is that below threshold the dot population ρ, and thus the gain, saturates as the injection current is increased as shown on Fig. 4. This effect is important in many current quantum dot devices as gain per unit length can be very low requiring device operation close to saturation. Transparency is reached when $\rho = 0.5$, and the threshold condition is obtained when $\rho = \rho_{\text{th}}$, where

$$\rho_{\text{th}} = \frac{1}{2\tau_s g_o \vartheta} + \frac{1}{2}. \tag{3}$$

A linear stability analysis is performed about the lasing fixed solution to understand how the system reacts to perturbations under different operating conditions. The eigenvalue solutions of the system, λ_n, determine the nature of the fixed point. In this case the solutions consist of two complex conjugate eigenvalues $\lambda_{1,2} = -\Gamma_a \pm i\Omega_a$, associated with the relaxation oscillations with damping Γ_a and oscillation frequency Ω_a. The third eigenvalue $\lambda_3 = -\Gamma_b$ is real and negative and associated with the capture mechanism into the dots. The damping rate of the relaxation oscillations as a function of the threshold occupation probability ρ_{th}, is shown in Fig. 2 for different capture rates. In each curve, there are three main features. If the laser operates close to transparency, (i.e if $\rho_{\text{th}} > \simeq 0.5$) the damping rate decreases as ρ_{th} increases. When $\rho_{\text{th}} \simeq 1$, the damping rate decreases rapidly. In the intermediate range, the damping as a function of ρ_{th} reaches a local minimum and then begins to increase until it reaches a local maximum close to $\rho_{\text{th}} = 1$. We can approximate the damping rate for two limiting cases. The first limit, shown in bold solid line in Fig. 5, corresponds to the limit of very high capture

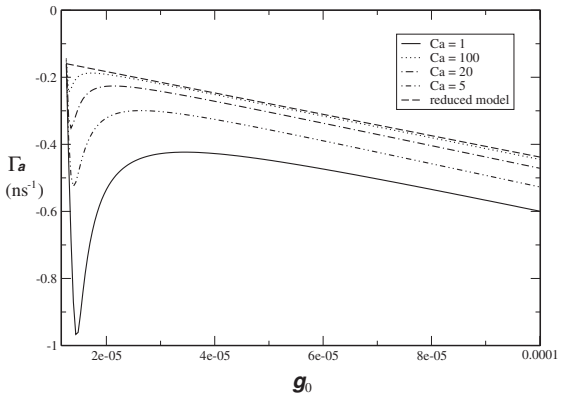

Fig. 5 Damping of relaxation oscillation as a function of g_0, for different values of the auger carrier capture rate C ($\times 10^{-20}$ m^4/s), and for the reduced equations in S and N, and S and ρ. For values of $g_0\vartheta < \dfrac{1}{\tau_s}$ the laser can never meet the lasing condition. (Other values as for Fig. 4).

rate of carriers from the well into the dots. Here, the dynamics of the well can be adiabatically eliminated and the laser can be described by the coupled rate equations for S and ρ and the relaxation oscillations can be easily calculated. The second limit is in the case where ρ_{th} is very close to one. Here Pauli blocking causes the carrier lifetime to be dominated by the lifetime in the well. In this case the damping rate can be calculated via the adiabatic elimination of ρ. Between these two limit cases, we note that the damping rate of the relaxation oscillations has a maxima.

In order to understand the behavior of the laser when subjected to optical feedback, it is worthwhile to first consider the behavior in both limits described above. In these cases, Eq. (2) can be reduced to a pair of equations, one describing the evolution of the field and the other describing the carriers, either N or ρ. In the first limit when N is adiabatically eliminated, the equations can be written as the Lang–Kobayashi equations. In the second limit, a similar though more complicated set of equations written in terms of E and N will emerge. In the analysis below, this will create non-linear effects leading to a renormalization of the relaxation oscillation. As shown above, the damping rate of the relaxation oscillations is an extremely important parameter for the sensitivity of semiconductor lasers with optical feedback. For quantum dot lasers, the sensitivity to optical feedback will therefore depend on ρ_{th}.

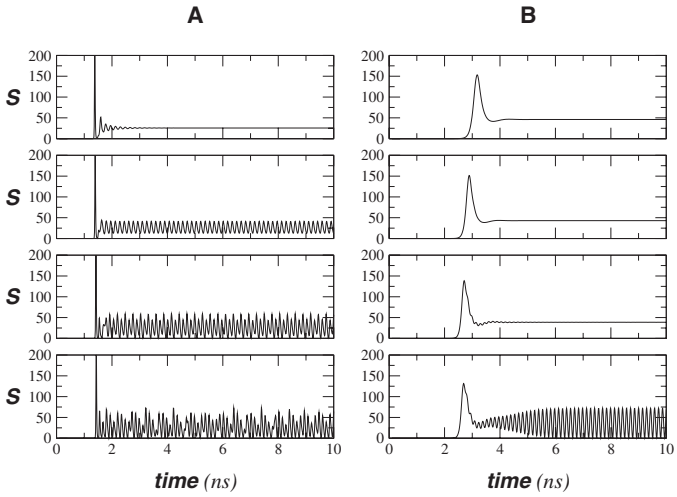

Fig. 6 Temporal behavior of lasers at different operating points subjected to different amounts of optical feedback, Photon density S ($\times 10^{18}$ m^{-3}) Vs time. Free running turnon transient top, with the feedback level increasing going down ($\gamma = 0$, 0.01, 0.02, 0.025 ps^{-1}). External cavity round trip time $\tau = 100$ ps. Operating point taken as 1.5 threshold. (Other values as for Fig. 4).

To illustrate this we choose two lasers operating with different ρ_{th}, labeled A and B on Fig. 4 and the rate Eq. (2) were numerically integrated. The lasing condition is reached at a slightly lower value of ρ_{th} with the introduction of optical feedback. The relaxation oscillations are more strongly damped for point B, which is operating close to the local maximum of the damping rate. The response to different amounts of optical feedback is shown in Fig. 6. In both cases the pump level was chosen to be 1.5 times the threshold current. The results presented in Fig. 6 were obtained for $\beta_1 = 0$ but similar results were obtained for $\beta_1 \neq 0$. In this case we took $\beta_1 \sim \rho_{th}/N_{th}$ to compare lasers with the same α factor at threshold. The turn on transients of the free running lasers as well as the response when subjected to optical feedback are shown in both cases. Laser A shows instabilities associated with optical feedback, displaying a self pulsating regime with a frequency of the external cavity round trip time. With increased feedback, period doubling of the undamped oscillation is observed and continues into a chaotic regime. Laser B is more stable as instabilities only appear for the highest feedback level shown here.

In summary, we have reviewed the main features of semiconductor lasers with optical feedback and presented new experimental results about the sensitivity of quantum dot semiconductor lasers with optical feedback. It was found that the damping rate of relaxation relaxation oscillations is the main source for the reduced sensitivity and this was illustrated with a rate equation model.

Acknowledgements This research was supported by Science Foundation Ireland under the grant SFI/01/F.1/CO13 the European Union in the framework of the IST-Dotcom, by the Irish Higher Education Authority under the Programme for Research in Third Level Institutions.

References

[1] D. Bimberg, M. Grundmann, and N. N. Ledentsov, Quantum Dot Heterostructures. Chichester, UK: Wiley, 1998.
[2] L. Zhang, R. Wang, Z. Zou, A. L. Gray, L. Olona, T. C. Newell, D. Webb, P. Varangis, and L. F. Lester, InAs Quantum dot DFB lasers on GaAs for uncooled 1310 nm fiber communication, OFC, (2003).
[3] D. O'Brien, S. Hegarty, G. Huyet, J. McInerney, D. Bimberg, C. Ribbat, V. Ustinov, A. Zhukov, S. Mikhrin, and A. R. Kovsh, Sensitivity to External Optical Feedback in Quantum Dot Lasers, submitted Elect. Lett., (2003).
[4] T. Newell, D. Bossert, A. Stintz, B. Fuchs, K. Malloy, and L. Lester, Gain and linewidth enhancement factor in InAs quantum-dot laser diodes, IEEE Phot. Tech. Lett. **11**, 1527 (1999).
[5] T. Morikawa, Y. Mitsuhashi, and J. Shimada, Elect. Lett. **112**, 435 (1976).
C. Risch and C. Voumard, J. Appl. Phys. **48**, 2083 (1977).
[6] D. Lenstra, M. V. Vaalen, and B. Jaskorzynska, Physica C **125**, 255 (1984).
[7] R. Lang and K. Kobayashi, IEEE J. Quantum Electron. **QE-16**, 347 (1980).
[8] R. Miles, A. Dandridge, A. Tveten, H. Taylor, and T. Giallorenzi, App. Phys. Lett. **37**, 990 (1980).
[9] L. Goldberg, H. F. Taylor, A. Dandridge, J. F. Weller, and R. Miles, IEEE J. Quantum Electron. **QE-18**, 555 (1982).
[10] F. Favre, D. L. Guen, and J. C. Simon, IEEE J. Quantum Electron. **QE-18**, 1712 (1982).
[11] G. P. Agrawal, IEEE J. Quantum Electron. **QE-20**, 468 (1984).
[12] K. E. Stubkajaer and M. B. Small, IEEE J. Quantum Electron. **QE-20**, 472 (1984).
[13] T. Fujita, S. Ishizuka, K. Fujito, H. Serizawa, and H. Sato, IEEE J. Quantum Electron. **QE-20**, 492 (1984).
[14] H. Temkin, N. A. Olsson, J. H. Abeles, R. A. Logan, and M. B. Panish, IEEE J. Quantum Electron. **QE-22**, 286 (1986).
[15] D. Lenstra, M. V. Vaalen, and B. Jaskorzynska, Physica C **125**, 255 (1984).
[16] R. Tkach and A. R. Chraplyvy, J. Lightwave Technol. **4**, 1655 (1986).
[17] P. Besnard, B. Meziane, and G. Stephan, IEEE J. Quantum Electron. **QE-29**, 1271 (1993).
[18] M. Giudici, C. K. Green, G. Giacomelli, U. Nespolo, and J. R. Tredicce, Phys. Rev. E **55**, 6414 (1997).
[19] T. Heil, I. Fischer, and W. Elsaesser, Phys. Rev. A **58**, R2672 (1998).
[20] B. Tromborg, J. H. Osmundsen, and H. Olesen, IEEE J. Quantum Electron. **QE-20**, 1023 (1984).
[21] J. Helms and K. Petermann, IEEE J. Quantum Electron. **QE-26**, 833 (1990).
[22] A. Ritter and H. Haug, J. Opt. Soc. Am. B **10**, 130 (1993).
[23] A. Levine, G. van Tartwijk, D. Lenstra, and T. Erneux, Phys. Rev. A **52**, R3436 (1995).

[24] G. Lythe, T. Erneux, A. Gavrielides, and V. Kovanis, Phys. Rev. A **55**, 4443 (1997).
[25] T. Sano, Phys. Rev. A **50**, 2719 (1994).
[26] G. van Tartwijk, A. Levine, and D. Lenstra, IEEE Sel. Top. Quantum Electron. **1**, 466 (1995).
[27] G. Huyet, P. Porta, S. P. Hegarty, J. McInerney, and F. Holland, A low dimension dynamical system to describe low-frequency fluctuations in a semiconductor laser with optical feedback, Opt. Commun. **180**, 339 (2000).
[28] I. Fischer, G. van Tartwijk, A. Levine, W. Elsaesser, E. O. Gobel, and D. Lenstra, Phys. Rev. Lett. **76**, 220 (1996).
[29] G. Huyet, S. Hegarty, M. Giudici, B. de Bruyn, and J. G. McInerney, Europhys. Lett. **40**, 619 (1997).
[30] G. Vaschenko, M. Giudici, J. Roca, C. Menoni, J. Tredicce, and S. Balle, Phys. Rev. Lett. **81**, 5536 (1998).
[31] G. Huyet, J. K. White, A. J. Kent, S. P. Hegarty, J. V. Moloney, and J. G. McInerney, Phys. Rev. A **60**, 1534 (1999).
[32] A. SpringThorpe, T. Garanzotis, P. Paddon, G. Pakulski, and K. I. White, Strained 1.3 μm mqw algainas lasers grown by digital alloy mbe, Electron. Lett. **36**, 1031 (2000).
[33] V. Ustinov, A. Zhukov, N. Maleev, A. Kovsh, S. Mikhrin, B. Volovik, Y. G. Musikhin, Y. Shernyakov, M. Maximov, A. Tsatsul'nikov, N. Ledenstov, Z. I. Alferov, J. Lott, and D. Bimberg, 1.3 μm inas/gaas quantum dot lasers and vcsels grown by molecular beam epitaxy, J. Cryst. Growth **227–228**, 1155 (2001).
[34] M. Kuntz, N. N. Ledentsov, D. Bimberg, A. R. Kovsh, V. M. Ustinov, A. E. Zhukov, and Y. M. Shernyakov, Spectrotemporal response of 1.3 μm quantum-dot lasers, Appl. Phys. Lett. **81**, 3846 (2002).
[35] A. Olsson and C. L. Tang, Coherent optical interference effects in external-cavity semiconductor lasers, IEEE J. Quantum Electron. **17**, 1320 (1981).
[36] L. A. Coldren and S. W. Corzine, Diode lasers and photonic integrated circuits. New York: Wiley Interscience, 1995.
[37] B. Krauskopf and D. Lenstra, Fundamental issues of nonlinear laser dynamics. Melville, New York: AIP, 2000.
[38] M. Sugawara, K. Mukai, and H. Shoji, Effect of phonon bottleneck on quantum-dot laser performance, Appl. Phys. Lett. **71**, 2791 (1997).
[39] A. Uskov, I. Magnusdottir, B. Tromborg, J. Mork, and R. Land, Line broadening caused by Coulomb carrier-carrier correlations and dynamics of carrier capture and emission in quantum dots, Appl. Phys. Lett. **79**, 1679 (2001).
[40] A. Uskov, Y. Boucher, J. L. Bihan, and J. McInerney, Theory of a self-assembled quantum-dot semiconductor laser with Auger carrier capture: Quantum efficiency and nonlinear gain, Appl. Phys. Lett. **11**, 1499 (1998).